

# **A nonintegrable discrete nonlinear Schrödinger equation with nonlinear hopping**

Zuo-Nong Zhu

Department of Mathematics, Shanghai Jiao Tong University, China

(This is a joint work with Liyuan Ma and Jialiang Ji)

International Workshop on Integrable Systems  
Mathematical Analysis and Scientific Computing  
October 17 - 21, 2015  
CASTS, National Taiwan University, Taipei

- Nonlinear Schrödinger equation (NLS)

$$iq_t + q_{xx} \pm 2|q|^2q = 0 \quad (1)$$

has received a wide study since the appearance of the work by Zakharov and Shabat (1972). NLS is a completely integrable system. It plays an important role in a wide range of physical subjects such as water waves, nonlinear optics, and plasma physics.

- Herbst and Ablowitz (PRL, 1989) investigated the discretizations

of NLS ( under the periodic boundary conditions:  $q_{n+N} = q_n$ )

$$iq_{n,t} + \frac{q_{n+1} + q_{n-1} - 2q_n}{h^2} + |q_n|^2(q_{n+1} + q_{n-1}) = 0, \quad (2)$$

$$iq_{n,t} + \frac{q_{n+1} + q_{n-1} - 2q_n}{h^2} + 2|q_n|^2q_n = 0. \quad (3)$$

It has been shown that the difference between two discrete schemes is only in the discretization of the nonlinear term, yet they have very different properties. The scheme (2) is integrable. This system has been demonstrated to be solvable by IST, and there is an infinite number of conserved quantities. Computations showed that the scheme (2) provides an excellent numerical scheme. However, the scheme (3) is nonintegrable. It produces chaotic solution for

intermediate levels of mesh refinement. But chaos disappears when the discretization is fine enough and convergence to a quasiperiodic solution is obtained.

- In this talk, we will address the spatial properties and numerical approximations of stationary and travelling solitary waves for a nonintegrable discrete NLS equation with nonlinear hopping:

$$iq_{n,t} + q_{n+1} + q_{n-1} - 2q_n + f(q_{n-1}, q_n, q_{n+1}) = 0, \quad (4)$$

where

$$\begin{aligned} f(q_{n-1}, q_n, q_{n+1}) = & \mu|q_n|^2(q_{n+1} + q_{n-1}) + \alpha q_n(\bar{q}_{n+1}q_{n-1} + q_{n+1}\bar{q}_{n-1}) \\ & + \beta q_n^2(\bar{q}_{n+1} + \bar{q}_{n-1}) - 2\gamma|q_n|^2q_n, \end{aligned}$$

the parameters  $\mu, \alpha, \beta, \gamma$  are real and  $\mu + \alpha + \beta - \gamma > 0$  or  $\mu + \alpha + \beta - \gamma < 0$  corresponds to the focusing case or defocusing case, respectively.

## Outline

1. A recall on nonintegrable discrete NLS equations
2. Spatial properties of nonintegrable discrete NLS (4)
3. Numerical approximations of stationary and travelling solitary waves of nonintegrable discrete NLS (4)
4. Conclusions

## 1. A recall on nonintegrable discrete NLS equations

• Christodoulides and Joseph (1988, Opt. Lett) investigated a discrete self-focusing in nonlinear array of coupled waveguides. By using the formalism of coupled-mode theory and by considering only nearest-neighbor interaction, they showed that the electric field propagating in the  $n$ th waveguide obeys:

$$i\frac{\partial E_n}{\partial z} + \beta E_n + c(E_{n+1} + E_{n-1}) + \mu E_n(|E_{n+1}|^2 + |E_{n-1}|^2) + \lambda|E_n|^2 E_n = 0, \quad (5)$$

where the nonlinear term  $\lambda|E_n|^2 E_n$  describes the self-phase modulation that takes place in the  $n$ th waveguide, and the term  $\mu E_n(|E_{n+1}|^2 +$

$|E_{n-1}|^2$ ) arises from the nonlinear overlap of the adjacent modes. In the real physics, the self-phase-modulation term dominates the nonlinear process, e.g.,  $\lambda \gg \mu$ . So they set  $\mu = 0$ , and discussed the noninterchangeable discrete NLS:

$$i\frac{\partial E_n}{\partial z} + c(E_{n+1} + E_{n-1} - 2E_n) + \lambda|E_n|^2 E_n = 0. \quad (6)$$

This model is also proposed by Davydov (1973) in biophysics for explain some of the fundamental questions, such as transfer, storage, and movement of vibrational energy in polypeptides.

- Herbst and Ablowitz (PRL, 1989) numerically studied noninte-

grable discrete NLS

$$i\frac{dq_n}{dt} + \frac{q_{n+1} + q_{n-1} - 2q_n}{h^2} + \gamma|q_n|^2q_n = 0 \quad (7)$$

with a periodic boundary condition  $q_{n+N} = q_n$ . The Hamiltonian structure of the scheme is given by the Hamiltonian

$$H = \sum_{n \in \mathbb{Z}} \left( \frac{|q_{n+1} - q_n|^2}{h^2} - \frac{\gamma}{2}|q_n|^4 \right) \quad (8)$$

The scheme conserves the norm

$$N = \sum_{n \in \mathbb{Z}} |q_n|^2 \quad (9)$$

The norm has a clear physical meaning being proportional to the total light power in the case of coupled optical waveguides or the

number of particles in a BEC. The discrete scheme produces chaotic solutions. However, chaos disappears when the discretization is fine enough and convergence to a quasiperiodic solution is obtained.

- A nonintegrable discrete NLS equation

$$\begin{aligned}
 & i q_{n,t} + q_{n+1} + q_{n-1} - 2q_n \\
 & + \mu |q_n|^2 (q_{n+1} + q_{n-1}) - \gamma |q_n|^2 q_n = 0, \quad \gamma \neq 0 \quad (10)
 \end{aligned}$$

was discussed by Cai, Bishop and Gronbech-Jensen (PRL, 1994).

- For the stationary discrete NLS

$$\phi_{n+1} = \frac{E + \gamma |\phi_n|^2}{1 + \mu |\phi_n|^2} \phi_n - \phi_{n-1}. \quad (11)$$

Dynamics including stability, solutions, wave transmission, and period-

doubling bifurcation for the discrete map are investigated (Hennig, Sun, Gabriel, Tsironis, Phys Rev E, 1995).

- By using discrete Fourier transformation, Ablowitz and Mussli-  
mani (Phys Rev E, 2002) investigated stationary and traveling soli-  
tary wave of dNLS

$$i\frac{\partial q_n}{\partial z} + \frac{q_{n+1} + q_{n-1} - 2q_n}{h^2} + |q_n|^2 q_n = 0. \quad (12)$$

- As we known, for dNLS, since both the translational and Gallileo  
invariances are broken, existence of a stationary solution

$$u_n(t) = \phi(hn)e^{i\omega t}$$

does not guarantee existence of a travelling solution

$$u_n(t) = \phi(hn - 2ct)e^{i\omega t}$$

Pelinovsky (Nonlinearity, 2006) derived a general four-parameter family of translationally invariant NLS lattice characterized by

$$i\frac{du_n}{dt} + \frac{u_{n+1} - 2u_n + u_{n-1}}{h^2} + f(u_{n-1}, u_n, u_{n+1}) = 0, \quad (13)$$

where  $f(u_{n-1}, u_n, u_{n+1})$  is represented by the four-parameter fam-

ily of cubic polynomials,

$$\begin{aligned}
f &= (1 - \chi - 4\xi - 2\eta)|u_n|^2(u_{n+1} + u_{n-1}) + \chi u_n^2(\bar{u}_{n+1} + \bar{u}_{n-1}) \\
&+ \xi[(2|u_n|^2 + |u_{n+1}|^2 + |u_{n-1}|^2)u_n + (\bar{u}_{n+1}u_{n-1} + u_{n+1}\bar{u}_{n-1})u_n \\
&+ (u_{n+1}^2 + u_{n-1}^2)\bar{u}_n] \\
&+ \eta(u_{n+1}^2 + u_{n-1}^2)(u_{n+1} + u_{n-1}) + \nu[u_{n+1}^2\bar{u}_{n-1} + u_{n-1}^2\bar{u}_{n+1} \\
&- |u_{n+1}|^2u_{n-1} - |u_{n-1}|^2u_{n+1}]
\end{aligned}$$

**Remark** Direct substitutions of the stationary solution and travelling solution to the discrete NLS show that  $\phi_n = \phi(hn)$  satisfies

the second-order difference eq,

$$\frac{\phi_{n+1} - 2\phi_n + \phi_{n-1}}{h^2} - \omega\phi_n + f(\phi_{n-1}, \phi_n, \phi_{n+1}) = 0,$$

while the function  $\phi(z) = \phi(hn - 2ct)$  satisfies the differential advance-delay eq,

$$2ic \frac{d\phi(z)}{dz} = \frac{\phi(z+h) - 2\phi(z) + \phi(z-h)}{h^2} - \omega\phi(z) + f(\phi(z-h), \phi(z), \phi(z+h)).$$

The stationary solution of the second-order difference eq is said to be translationally invariant if the function  $\phi_n$  can be extended to a one-parameter family of continuous solutions  $\phi(z-s)$  on  $z \in R$  of the differential advance-delay eq with  $c = 0$ . It has been shown

that the discrete NLS lattice conserves the momentum  $M$  invariant,

$$M = i \sum_{n \in \mathbb{Z}} (\bar{u}_{n+1} u_n - u_{n+1} \bar{u}_n)$$

has no Hamiltonian structure, and may possess the power  $N$  invariant,

$$N = \sum_{n \in \mathbb{Z}} (|u_n|^2 + \bar{u}_{n+1} u_n + u_{n+1} \bar{u}_n)$$

if  $\nu = 0$  and

$$\begin{aligned} (a) \chi = \xi = 0, & \quad (b) \chi = 0, \xi = \frac{1}{4} - \eta, \\ (c) \xi = \eta = 0, & \quad (d) \eta = 0, \chi = \frac{1}{2} - 2\xi \end{aligned}$$

## **2. Spatial properties of nonintegrable discrete NLS (4)**

In this talk, by using the planar nonlinear dynamical map approach, we will address spatial properties of nonintegrable discrete NLS (4). By using discrete Fourier transformation method, we will obtain numerical approximations of stationary and travelling solitary wave solutions for the nonintegrable discrete NLS equation.

We will emphasize that nonintegrable dNLS equation (4) can not be obtained by the reduction of nonintegrable dNLS equation (13) with (14), and the properties of equation (4) differ from the ones of equation (13), e.g., equation (4) has no conserved momentum  $M$

and conserved power  $N$ .

**(2.1) A planar nonlinear dynamical map related to nonintegrable discrete NLS (4)**

Set  $q_n(t) = \varphi_n e^{i(F-2)t}$ , eq. (4) is converted into the stationary dNLS equation:

$$\begin{aligned}
 & -F\varphi_n + (1 + \mu|\varphi_n|^2)(\varphi_{n+1} + \varphi_{n-1}) - 2\gamma|\varphi_n|^2\varphi_n \\
 & + \alpha(\bar{\varphi}_{n+1}\varphi_{n-1} + \varphi_{n+1}\bar{\varphi}_{n-1})\varphi_n + \beta\varphi_n^2(\bar{\varphi}_{n+1} + \bar{\varphi}_{n-1}) = 0.
 \end{aligned}
 \tag{14}$$

Let  $\varphi_n = r_n e^{i\theta_n}$ , we rewrite equation (14) as

$$\frac{r_{n+1} \cos(\Delta\theta_{n+1}) + r_{n-1} \cos(\Delta\theta_n) = (F + 2\gamma r_n^2)r_n - 2\alpha r_{n+1}r_n r_{n-1} \cos(\Delta\theta_{n+1} + \Delta\theta_n)}{1 + (\mu + \beta)r_n^2}, \quad (15)$$

and

$$r_{n+1} \sin(\Delta\theta_{n+1}) - r_{n-1} \sin(\Delta\theta_n) = 0, \quad (16)$$

where  $\Delta\theta_n = \theta_n - \theta_{n-1}$ . Eq.(16) implies a conserved quantity:

$$J = r_n r_{n-1} \sin(\Delta\theta_n). \quad (17)$$

Through introducing real-valued variables transformations:

$$\begin{cases} x_n = \bar{\varphi}_n \varphi_{n-1} + \varphi_n \bar{\varphi}_{n-1} = 2r_n r_{n-1} \cos(\Delta\theta_n), \\ y_n = i[\bar{\varphi}_n \varphi_{n-1} - \varphi_n \bar{\varphi}_{n-1}] = 2J, \\ z_n = |\varphi_n|^2 - |\varphi_{n-1}|^2 = r_n^2 - r_{n-1}^2, \end{cases} \quad (18)$$

equations (15) and (16) yield a plane map  $M_{\alpha,\beta,\gamma,F,J}$

$$M_{\alpha,\beta,\gamma,F,J} : \begin{cases} x_{n+1} = \frac{(F + \gamma(\omega_n + z_n))(\omega_n + z_n) + 4\alpha J^2 - x_n \left(1 + \frac{\mu + \beta}{2}(\omega_n + z_n)\right)}{1 + \frac{\mu + \beta}{2}(\omega_n + z_n) + \alpha x_n}, \\ z_{n+1} = \frac{x_{n+1}^2 - x_n^2}{2(\omega_n + z_n)} - z_n, \end{cases} \quad (19)$$

with  $\omega_n = \sqrt{x_n^2 + z_n^2 + 4J^2}$ .

## (2.2) Exact period orbits of the map (19)

### Case 1: $J = 0$

Considering the peculiar orbit with  $z_n = 0, \forall n$ , we obtain  $x_{n+1} = \pm x_n, \forall n$ . This means that the period-1 orbit and the period-2 orbit to the map (19) are constructed. The period-1 orbit is the fixed point of the two-dimensional real map (19),

$$x = x_0 = \frac{F - 2}{\mu + \alpha + \beta - \gamma} > 0, \quad z = 0, \quad (20)$$

or

$$x = x_0 = \frac{F + 2}{\mu + \beta + \gamma - \alpha} < 0, \quad z = 0. \quad (21)$$

The period-2 orbit is

$$x = x_0 = \frac{-F}{\alpha + \gamma} > 0, \quad z = 0, \quad (22)$$

or

$$x = x_0 = \frac{F}{\alpha + \gamma} < 0, \quad z = 0, \quad (23)$$

which creates period-doubling bifurcation for the map (19).

### **Case 2: $J \neq 0$**

We introduce the following scaling transformation:  $x_n = 2J\tilde{x}_n$ ,  $z_n = 2J\tilde{z}_n$ ,  $J\gamma = \tilde{\gamma}$  and  $\omega_n = 2J\tilde{\omega}_n$ , then the new variable map is rewrit-

ten as,

$$M_{\alpha,\beta,\tilde{\gamma},F,J} : \begin{cases} \tilde{x}_{n+1} = \frac{(F+2\tilde{\gamma}(\tilde{\omega}_n+\tilde{z}_n))(\tilde{\omega}_n+\tilde{z}_n)+2\alpha J-\tilde{x}_n(1+J(\mu+\beta)(\tilde{\omega}_n+\tilde{z}_n))}{1+J(\mu+\beta)(\tilde{\omega}_n+\tilde{z}_n)+2\alpha J\tilde{x}_n}, \\ \tilde{z}_{n+1} = \frac{\tilde{x}_{n+1}^2-\tilde{x}_n^2}{2(\tilde{\omega}_n+\tilde{z}_n)} - \tilde{z}_n, \end{cases} \quad (24)$$

with  $\tilde{\omega}_n = \sqrt{\tilde{x}_n^2 + \tilde{z}_n^2 + 1}$  as  $J > 0$ , or  $\tilde{\omega}_n = -\sqrt{\tilde{x}_n^2 + \tilde{z}_n^2 + 1}$  as  $J < 0$ .

Set  $\tilde{z}_n = 0, \forall n$ , we get  $\tilde{x}_{n+1} = \tilde{x}_n$ , i.e.,  $\tilde{x}_n$  is the period-1 orbit, and  $\tilde{x}_{n+1} = -\tilde{x}_n$ , i.e.  $\tilde{x}_n$  is the period-2 orbit. The period-1 orbit

is determined by

$$2J(\gamma - \alpha)x^2 - 2x - 2J(\mu + \beta)x\omega + F\omega + 2J(\alpha + \gamma) = 0, \quad z = 0 \quad (25)$$

where  $\omega = \pm\sqrt{1 + x^2}$ . Considering a special case  $\alpha + \gamma = 0$  and  $F = 0$ , we have

$$2\alpha Jx \pm J(\mu + \beta)\sqrt{1 + x^2} + 1 = 0, \quad z = 0.$$

When  $\text{sgn}(2\alpha Jx + 1) = \text{sgn}(\pm J(\mu + \beta)\sqrt{1 + x^2})$  and  $1 + J^2(4\alpha^2 - (\mu + \beta)^2) \geq 0$ , the exact period-1 orbit solution is

given by

$$x = \tilde{x}_0 = \frac{-2\alpha \pm (\mu + \beta) \sqrt{1 + J^2 (4\alpha^2 - (\mu + \beta)^2)}}{J (4\alpha^2 - (\mu + \beta)^2)}, \quad z = 0 \quad (26)$$

When  $\frac{-F}{J(\alpha+\gamma)} > 0$ , and  $|F| > 2|J(\alpha + \gamma)|$ , the period-2 orbits are

$$x = \tilde{x}_0 = \sqrt{\frac{F^2}{4J^2(\alpha + \gamma)^2} - 1}, \quad z = 0. \quad (27)$$

or

$$x = \tilde{x}_0 = -\sqrt{\frac{F^2}{4J^2(\alpha + \gamma)^2} - 1}, \quad z = 0. \quad (28)$$

## 2.3 Stability of orbits of the plane map

The stability of an orbit of period  $l$  of a plane map  $M$  has been discussed (Greene, 1968; Hennig, Sun, Gabriel, Tsironis, 1995; Hennig, Rasmussen, Gabriel, Bülow, 1996, 1997). Suppose the plane map  $M$  has the general form

$$x_1 = f(x_0, z_0), \quad z_1 = g(x_0, z_0). \quad (29)$$

Stability of an orbit of period  $l$  around a fixed point  $(x^*, z^*)$  of the map  $M$  is determined by its residue

$$\rho = \frac{1}{4} \left( 2 - \text{Tr}(\Pi_{j=1}^l DM^{(j)}(x^*, z^*)) \right), \quad (30)$$

where  $DM(x^*, z^*)$  is the tangent map of  $M$  at  $(x^*, z^*)$  defined by

$\frac{\partial(f,g)}{\partial(x,z)}|_{(x^*,z^*)}$ . The periodic orbit is stable when  $0 < \rho < 1$  (elliptic) and unstable when  $\rho > 1$  (hyperbolic) or  $\rho < 0$  (hyperbolic).

### Case 1: $J = 0$

For the fixed point (20), the residue is

$$\rho = \frac{(F - 2)(\alpha + \beta + \mu - \gamma)}{F(2\alpha + \beta + \mu) - 2(\alpha + \gamma)}. \quad (31)$$

So the stability properties of the fixed point (20) are

(i)  $0 < \rho < 1$  (elliptic),  $F(2\alpha + \beta + \mu) > 2(\alpha + \gamma)$  and  $F(\alpha + \gamma) + 2(\beta + \mu - 2\gamma) > 0$ ;

(ii)  $\rho > 1$  (hyperbolic),  $F(2\alpha + \beta + \mu) > 2(\alpha + \gamma)$  and  $F(\alpha + \gamma) + 2(\beta + \mu - 2\gamma) < 0$ ;

(iii)  $\rho < 0$  (hyperbolic),  $F(2\alpha + \beta + \mu) < 2(\alpha + \gamma)$ .

• In case (i) the fixed point (20) is a stable elliptic point encircled by stable elliptic type map orbits. (e.g.,  $F > 2$  and  $0 < \alpha + \gamma < 2\alpha + \beta + \mu$ , the residue satisfies  $0 < \rho < 1$ ).

The fig.1 (a) describes the orbits around the stable elliptic point where the parameters are  $F = 4, \alpha = \mu = 1, \beta = \gamma = 0.5$  and initial value  $(x_1, z_1) = (j, 0) (0.1 \leq j \leq 1.5)$  with an interval 0.1.

The fixed point is  $(x^*, z^*) = (1, 0)$  and  $\rho = \frac{4}{11}$ .

• In the cases (ii) and (iii), fixed point  $(x^*, 0)$  becomes an unstable hyperbolic point. In the particular conditions  $F < 2$  and

$0 < 2\alpha + \beta + \mu < \alpha + \gamma$ , we have  $\rho < 0$ . The unstable orbits related to the hyperbolic point  $(x^*, z^*) = (1, 0)$  are shown in fig.1 (b) for parameters  $F = 1.7, \alpha = 1, \beta = -2, \gamma = 0.3, \mu = 1$  and initial value  $(x_1, z_1) = (j, 0)(0.1 \leq j \leq 1)$  with interval 0.06, and fig.1 (c) where initial value  $(x_1, z_1) = (j, 0)(1.05 \leq j \leq 1.5)$  with interval 0.06. The fig. 1(e) describes the unstable orbits in the neighborhood of the hyperbolic point  $(x^*, 0) = (1.125, 0)$ , where we choose parameters  $F = 0.2, \alpha = -2, \beta = 0.2, \gamma = 0.3, \mu = 0.5$  such that the residue  $\rho > 1$ , and initial values  $(x_1, z_1) = (j, 0)(0 \leq j \leq 1.2)$  with interval 0.03.

The residue for the fixed point (21) is

$$\rho = \frac{(F + 2)(\alpha - \beta - \mu - \gamma)}{F(2\alpha - \beta - \mu) + 2(\alpha + \gamma)}. \quad (32)$$

So the stability properties of the fixed point (21) are

(i)  $0 < \rho < 1$  (elliptic),  $F(2\alpha - \beta - \mu) + 2(\alpha + \gamma) > 0$ , and  $F(\alpha + \gamma) + 2(\beta + \mu + 2\gamma) > 0$ ;

(ii)  $\rho > 1$  (hyperbolic),  $F(2\alpha - \beta - \mu) + 2(\alpha + \gamma) > 0$ , and  $F(\alpha + \gamma) + 2(\beta + \mu + 2\gamma) < 0$ ;

(iii)  $\rho < 0$  (hyperbolic),  $F(2\alpha - \beta - \mu) + 2(\alpha + \gamma) < 0$ .

In the following particular conditions:

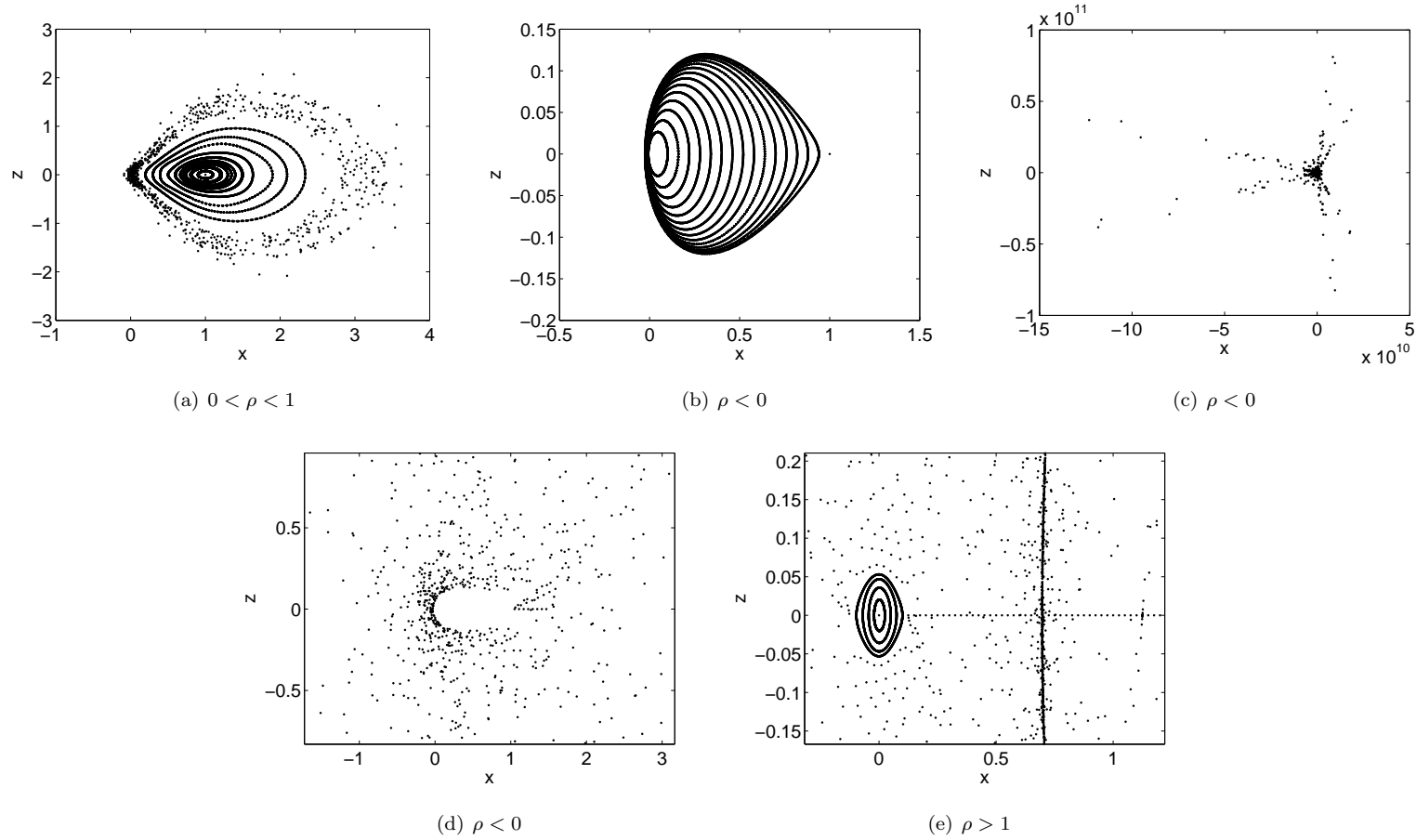


Figure 1: Map orbits related to (a): the stable elliptic point  $(x, z) = (1, 0)$ . Parameters:  $F = 4, \alpha = \mu = 1, \beta = \gamma = 0.5$  and initial value  $(x_1, z_1) = (j, 0) (0.1 \leq j \leq 1.5)$  with an interval 0.1. Chaotic behavior appears at  $(x_1, z_1) = (0.1, 0)$ . (b): the hyperbolic point  $(x, z) = (1, 0)$  when the parameters  $F = 1.7, \alpha = 1, \beta = -2, \gamma = 0.3, \mu = 1$  and initial value  $(x_1, z_1) = (j, 0) (0.1 \leq j \leq 1)$  with interval 0.06. (c): initial value  $(x_1, z_1) = (j, 0) (1.05 \leq j \leq 1.5)$  with interval 0.06. (d): the local of (c). (e): the hyperbolic point  $(x, z) = (1.125, 0)$  where  $F = 0.2, \alpha = -2, \beta = 0.2, \gamma = 0.3, \mu = 0.5$  and  $(x_1, z_1) = (j, 0) (0 \leq j \leq 1.2)$  with interval 0.025.

(i) When  $F < -2$  and  $2\alpha - \beta - \mu < \alpha + \gamma < 0$ , e.g.,  $F = -3$ ,  $\alpha = 1$ ,  $\beta = 3$ ,  $\gamma = -2$  and  $\mu = 1$ , we obtain the residue  $\rho = 0.25$  and the stable elliptic point  $(x^*, 0) = (-1, 0)$ . The orbits of the map emerging chaotic property are shown in fig.2.

(ii)  $F > -2$  and  $\alpha + \gamma < 2\alpha - \beta - \mu < 0$ ,  $\rho < 0$  (hyperbolic).

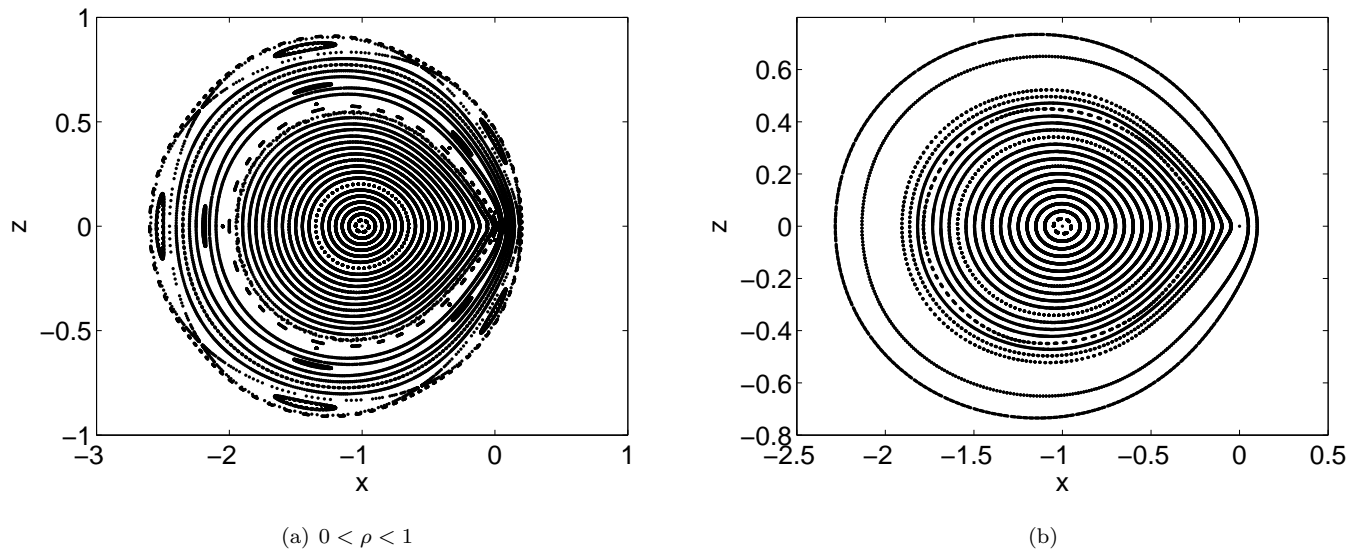


Figure 2: Map orbits related to the stable elliptic point  $(x, z) = (-1, 0)$ . Parameters:  $F = -3, \alpha = 1, \beta = 3, \gamma = -2, \mu = 1$  and initial value  $(x_1, z_1) = (j, 0) (-2.6 \leq j \leq -1)$  with an interval 0.05. The chaotic layer is clearly shown. (b): initial value  $(x_1, z_1) = (j, 0) (-1 \leq j \leq 0.1)$  with an interval 0.05.

## Case 2: $J \neq 0$

Set  $\Delta = \sqrt{4\alpha^2 J^2 + 2\alpha J\omega(F + 2\tilde{\gamma}\omega) + (1 + J\omega(\mu + \beta))^2}$ . The

residue corresponding to (25) is given by

$$\rho = \frac{1}{8} \left( 6 + \frac{c_1\omega^4 + c_2\omega^3 + c_3\omega^2 + c_4\omega + c_5}{\alpha J\omega\Delta^3} \right), \quad (33)$$

where

$$\begin{aligned}
c_1 &= 2J^4(\alpha + \gamma)(\beta + \mu) \left( 4\alpha\gamma + (\beta + \mu)^2 \right), \\
c_2 &= FJ^3(\beta + \mu)^3 + 2J^3(3\alpha + \gamma(3 - \Delta))(\beta + \mu)^2 + 4FJ^3\alpha(\alpha + 2\gamma)(\beta + \mu) \\
&\quad - 4J\alpha \left( 3\gamma^2\Delta + 2J\alpha\tilde{\gamma}(1 + \Delta) + J^2\alpha^2(2 + \Delta) \right), \\
c_3 &= 2J^2 \left( F^2\alpha + \left( 3 + 4J^2\alpha^2 \right) (\alpha + \gamma) - 2\gamma\Delta \right) (\beta + \mu) \\
&\quad - JF \left( 8\alpha\tilde{\gamma}\Delta + J \left( 4\alpha^2 + (\Delta - 3)(\beta + \mu)^2 \right) \right), \tag{34}
\end{aligned}$$

$$\begin{aligned}
c_4 &= 2\tilde{\gamma}(1 - \Delta) + 8J^2\alpha^2\tilde{\gamma}(1 + \Delta) + 4J^3\alpha^2(\alpha(2 + 4\Delta) + F(\beta + \mu)) \\
&\quad + J \left( \alpha \left( 2 - F^2\Delta \right) + F(3 - 2\Delta)(\beta + \mu) \right), \tag{35}
\end{aligned}$$

$$c_5 = F \left( 1 - \Delta + 4J^2\alpha^2(1 + \Delta) \right).$$

For special case  $\alpha + \gamma = 0$  and  $F = 0$ , the residues for 1-period orbit (26) are  $\rho = 1$ .

This means that we can not determine the stability of the orbit around the fixed point.

## **(2.4) Numerical simulation of orbits of the map (24)**

In the general case  $z_n \neq 0$ , we can not obtain exact orbit for map (24). Here we give a numerical simulation for the orbits of the map. In each figure, the space lattice site  $n$  takes the value from 1 to 1000, and the  $x$  and  $z$  axes denote the values of  $\tilde{x}_n$  and  $\tilde{z}_n$  ( $n = 1, 2, \dots, 1000$ ) of the map (24), respectively. In figs.3-7, we display that how the parameters  $\alpha$ ,  $\beta$  and  $\gamma$  affect the orbits of the map.

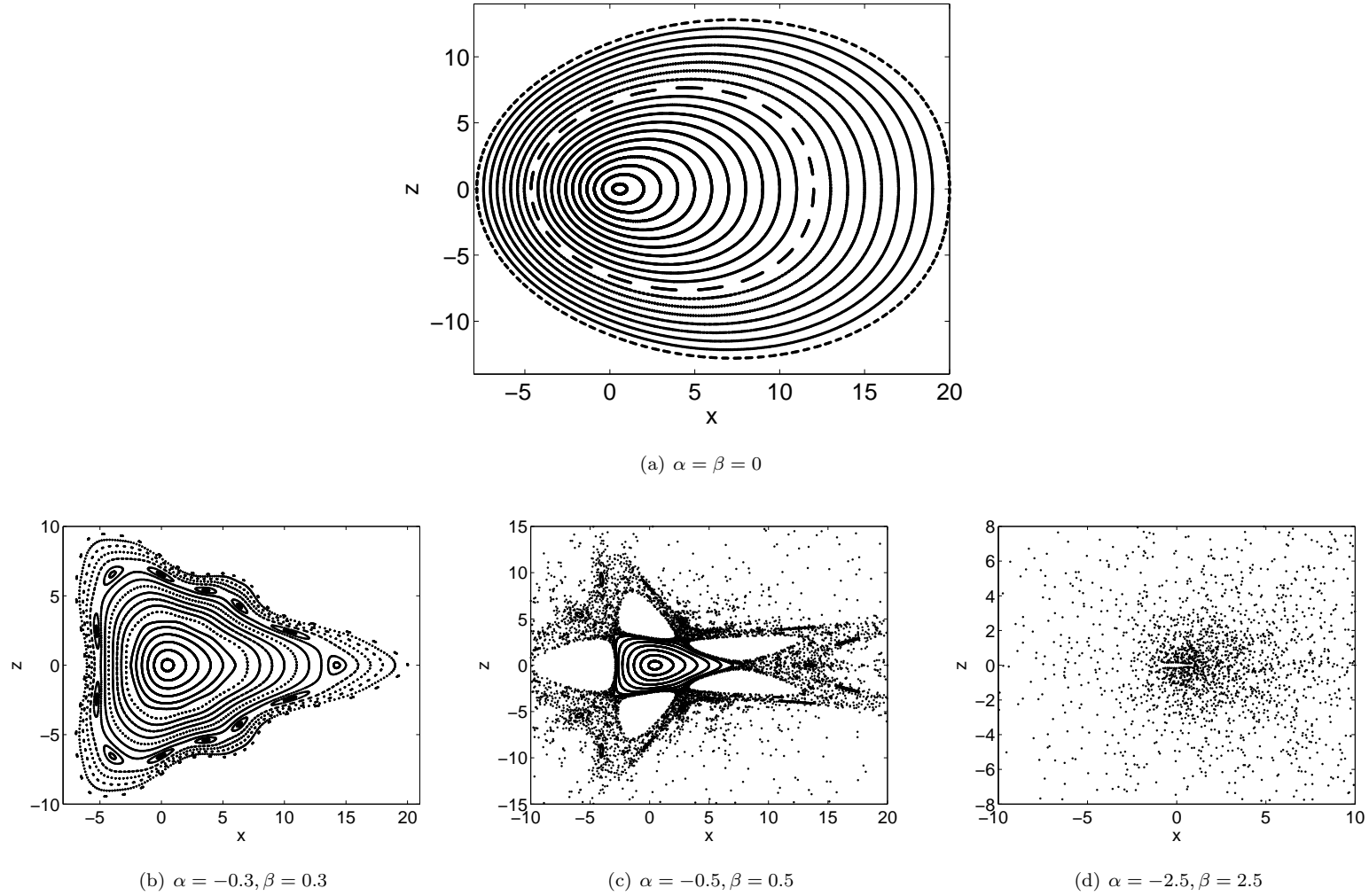
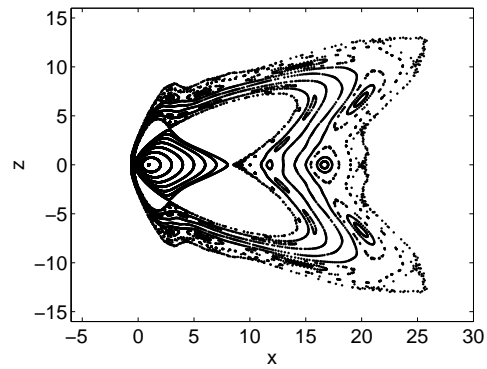
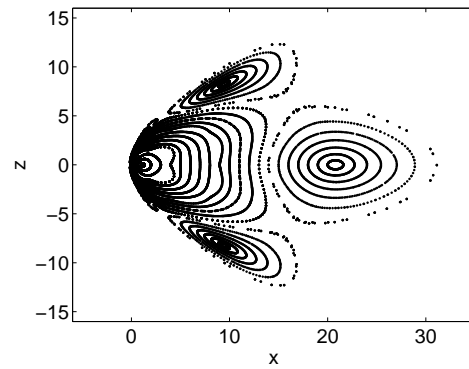


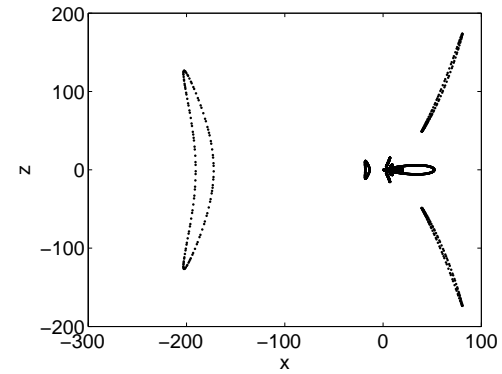
Figure 3: Constraint condition  $\mu + \alpha + \beta - \gamma = 1$  (focusing case).  $\gamma = \tilde{\gamma}/J$ . Orbits of the map  $M$  (24) with the parameters  $\tilde{\gamma} = 0.2, F = 1.0, J = 0.25, \mu = 1.8$ . (a) regular regime for the nonintegrable discrete NLS:  $\alpha = \beta = 0$ ; (b-d)  $\alpha < 0$ , the orbits disappear or evolve into chaotic as the parameter  $|\alpha| = |\beta|$  get larger. Initial value  $(x_1, z_1) = (j, 0) (1 \leq j \leq 20)$  with an interval of 1.



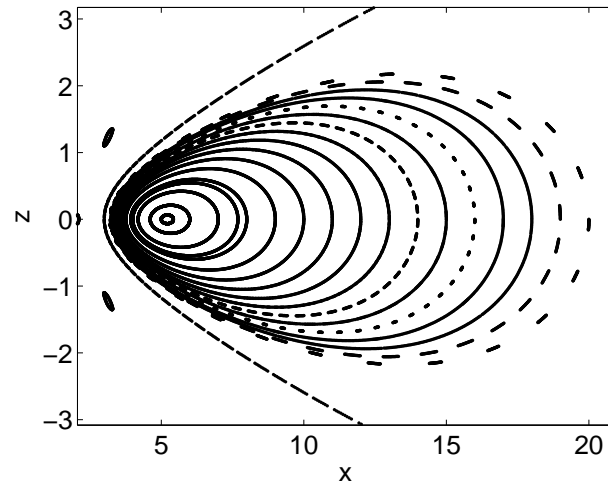
(a)  $\alpha = 1.35, \beta = -1.35$



(b)  $\alpha = 2, \beta = -2$



(c)  $\alpha = 25, \beta = -25$



(d) local of 2(d)

Figure 4: Constraint condition  $\mu + \alpha + \beta - \gamma = 1$  (focusing case).  $\gamma = \tilde{\gamma}/J$ . Orbits of the map  $M$  (24) with the parameters  $\tilde{\gamma} = 0.2, F = 1.0, J = 0.25, \mu = 1.8$ . (a-c)  $\alpha > 0$ , the orbits disappear or evolve into chaotic as the parameter  $|\alpha| = |\beta|$  get larger. Initial value  $(x_1, z_1) = (j, 0) (1 \leq j \leq 20)$  with an interval of 1.

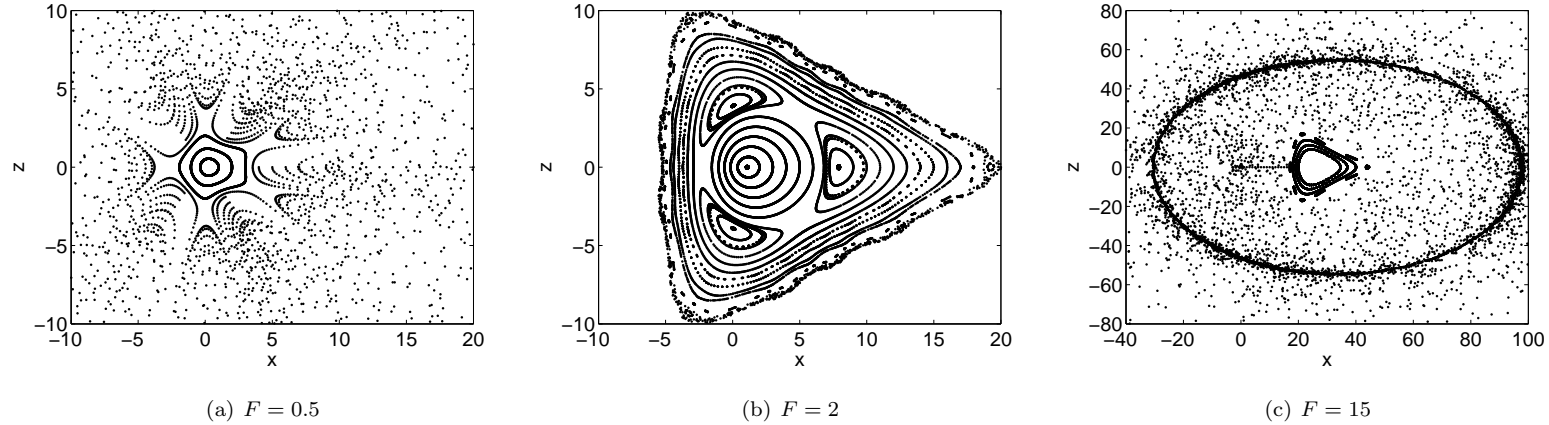


Figure 5: Constraint condition  $\mu + \alpha + \beta - \gamma = 1$  (focusing case).  $\gamma = \tilde{\gamma}/J$ . Effect of  $F$  on orbits of the map  $M$  (24) with the parameters  $\tilde{\gamma} = 0.2, J = 0.25, \mu = 1.8, \alpha = -\beta = -0.3$ . Initial value  $(x_1, z_1) = (j, 0) (1 \leq j \leq 20)$  with an interval of 1.

## (2.5) Exact spatial period solutions of nonintegrable dNLS equation

For the probability current  $J = 0$ , the period-1 orbit (20) yields a period-1 solution to the nonintegrable dNLS equation, i.e.,  $q_n(t) = \sqrt{\frac{x_0}{2}} e^{i[(F-2)t + \theta_0]}$ , where  $\theta_0$  is the argument of  $\varphi_0$ . However, for

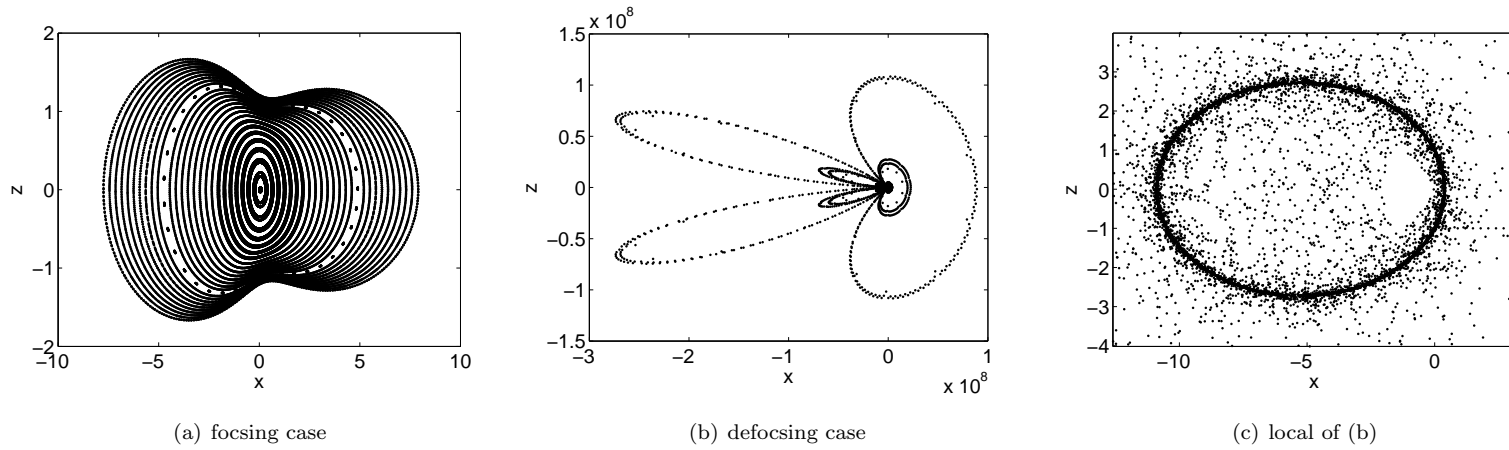


Figure 6: Orbits of the map  $M$  (24). (a): focusing case:  $F = 0.4, \tilde{\gamma} = -\alpha = 0.2, J = \mu = 1, \beta = 1.5$ . Initial value  $(x_1, z_1) = (j, 0) (-2 \leq j \leq 8)$  with an interval of 0.3.  $\mu + \alpha + \beta - \gamma = 2.1$ . (b):  $F = -1.3, \tilde{\gamma} = -\alpha = 0.2, J = 0.4, \mu = 1.2, \beta = -2$ . Initial value  $(x_1, z_1) = (j, -1) (0 \leq j \leq 5)$  with an interval of 0.3.  $\mu + \alpha + \beta - \gamma = -1.5$ .

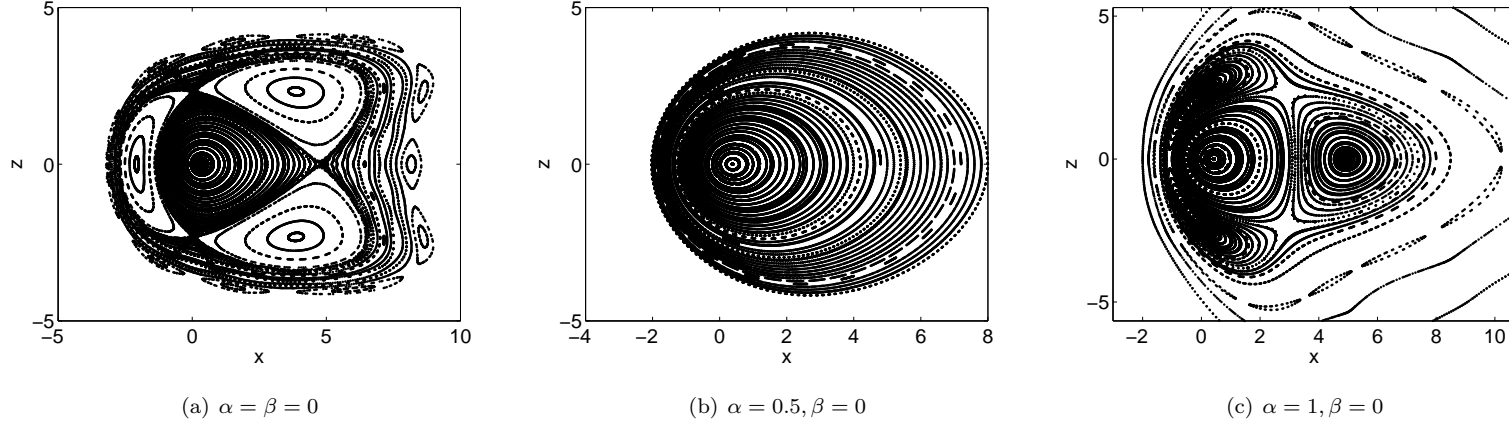


Figure 7: Orbits of the map  $M$  with the parameters  $F = 0.5, J = 0.1, \tilde{\gamma} = 0.2$  and  $(x_1, z_1) = (j, 0) (-2 \leq j \leq 8)$  with an interval of 0.2. (a) there are chaotic sea; (b-c) the effect of the parameter  $\alpha$  on chaotic sea.

another period-1 orbit (21), its corresponding solution is a period-2 solution,

$$\left\{ \begin{array}{l} q_0(t) = \sqrt{\frac{-x_0}{2}} e^{i[(F-2)t + \theta_0]}, \\ q_1(t) = -\sqrt{\frac{-x_0}{2}} e^{i[(F-2)t + \theta_0]}, \\ q_{n+2}(t) = q_n(t) \quad \forall n, \end{array} \right. \quad (36)$$

where  $x_0 = \frac{F+2}{\mu-\alpha+\beta+\gamma} < 0$ .

The period-2 orbit(22) gives the following period-4 solution to the nonintegrable dNLS equation

$$\begin{cases} q_0(t) = q_3(t) = \sqrt{\frac{x_0}{2}} e^{i[(F-2)t+\theta_0]}, \\ q_1(t) = q_2(t) = -\sqrt{\frac{x_0}{2}} e^{i[(F-2)t+\theta_0]}, \\ q_{n+4}(t) = q_n(t) \quad \forall n, \end{cases} \quad (37)$$

where  $x_0 = \frac{-F}{\alpha+\gamma} > 0$ . But, for another period-2 orbit, it can not yield the corresponding solution to nonintegrable dNLS equation.

For  $J \neq 0$ , when period-1 orbit  $x = \tilde{x}_0 > 0$ , the generating solution  $q_n(t) = r e^{i[(F-2)t+\theta_0+n \arcsin(J/r^2)]}$  to the nonintegrable dNLS e-

quation is given by the period-1 orbit (25), where  $r$  admits the constraint condition:  $J^2(1 + \tilde{x}_0^2) = r^4$ . It is not period in general. But when  $\arcsin \frac{J}{r^2} = \frac{2\pi}{m}$ ,  $\forall m \in \mathbb{Z}^+$  and  $m > 3$ , it is a period- $m$  solution. For the period-2 orbit (27), its yielding solution is a period-4 solution

$$q_n(t) = r e^{i \left( (F-2)t - \left[ \frac{n}{2} \right] \pi + \frac{1+(-1)^{n+1}}{2} \arcsin \frac{J}{r^2} \right)}. \quad (38)$$

Like the case of  $J = 0$ , in the case of  $J \neq 0$ , another period-2 orbit can not yield the corresponding solution to nonintegrable dNLS equation.

**Remark 1:** The periodicity of the orbits of the plane map does not coincide with the space periodicity of the solution. This is an interesting phenomenon for the nonintegrable dNLS equation (4).

**Remark 2:** The numerical simulations for the orbit of stationary dNLS equation (24) are given. However, the corresponding solutions of the nonintegrable dNLS equation (4) are still not clear.

### 3. Numerical approximations of stationary and travelling solitary waves of nonintegrable discrete NLS (4)

By using the discrete Fourier analysis approach ( Ablowitz and Muslimani, Phys. Rev. E, 2002), we will obtain numerical approximations of discrete stationary and traveling solitary wave solutions for nonintegrable dNLS equation (4) with the form

$$\begin{aligned} & i q_{n,z} + (1 + |q_n|^2)(q_{n+1} + q_{n-1}) - 2q_n \\ & + \alpha q_n(\bar{q}_{n+1}q_{n-1} + q_{n+1}\bar{q}_{n-1}) + \beta q_n^2(\bar{q}_{n+1} + \bar{q}_{n-1}) - \gamma |q_n|^2 q_n = 0. \end{aligned} \tag{39}$$

The key point of the method is to transform a differential advance-delay equation into an integral equation which can be solved by using numerical method.

Set

$$q_n(z) = u(\xi)e^{-i\psi_n}, \quad (40)$$

where  $\xi = nh - vz$ ,  $\psi_n = \delta nh - \omega z$  and  $u(\xi) = F(\xi) + iG(\xi)$  with  $v$  and  $\omega$  being the soliton velocity and wave-number shift, and  $h$

being the lattice spacing. Then eq. (39) can be written as

$$\begin{aligned}
& vG' - 2F + \left(1 + F^2 + G^2 + \beta(F^2 - G^2)\right) (\mathcal{D}_1F + \mathcal{D}_2G) - \gamma(F^2 + G^2)F \\
& + 2\beta FG(\mathcal{D}_1G - \mathcal{D}_2F) + 2\alpha F [((E_+F)(E_-F) + (E_+G)(E_-G)) \cos(2\delta h) \\
& + ((E_+G)(E_-F) - (E_+F)(E_-G)) \sin(2\delta h)] = \omega F, \\
& - vF' - 2G + \left(1 + F^2 + G^2 - \beta(F^2 - G^2)\right) (\mathcal{D}_1G - \mathcal{D}_2F) \\
& - \gamma(F^2 + G^2)G + 2\beta FG(\mathcal{D}_1F + \mathcal{D}_2G) \\
& + 2\alpha G [((E_+F)(E_-F) + (E_+G)(E_-G)) \cos(2\delta h) \tag{41} \\
& + ((E_+G)(E_-F) - (E_+F)(E_-G)) \sin(2\delta h)] = \omega G,
\end{aligned}$$

where

$$\mathcal{D}_1\mathcal{H} = \cos(\delta h)(E_+ + E_-)\mathcal{H}, \quad \mathcal{D}_2\mathcal{G} = \sin(\delta h)(E_+ - E_-)\mathcal{G}.$$

with  $E_{\pm}X(\xi) = X(\xi \pm h)$ .

Eq. (41) is a nonlinear differential advance-delay system. It is difficult to find a solution to this system. To find its solution, we employ the discrete Fourier transformation method:

$$\begin{aligned} \hat{\mathcal{F}}(q) &= \sum_{n=-\infty}^{+\infty} \mathcal{F}(nh)e^{-iqnh}, \\ \mathcal{F}(nh) &= \frac{h}{2\pi} \int_{-\pi/h}^{\pi/h} \hat{\mathcal{F}}(q)e^{iqnh} dq. \end{aligned} \quad (42)$$

• Remarks: (1) As  $h \rightarrow 0$ , the discrete Fourier transform  $\Rightarrow$  continuous Fourier transform.

(2) The discrete Fourier transform possesses the same properties of continuous Fourier transform, e.g.,

$$\begin{aligned}\mathcal{F}[f'(x)] &= -iq\mathcal{F}[f(x)] \\ \mathcal{F}[f_1f_2] &= \frac{h}{2\pi}\mathcal{F}[f_1] * \mathcal{F}[f_2]\end{aligned}$$

Eq. (41) can be regarded as a nonlinear integral equation:

$$\begin{aligned}\hat{F}(q) &= \frac{\Omega_1(q)Q_1[\hat{F}, \tilde{G}](q) + \Omega_2(q)Q_2[\hat{F}, \tilde{G}](q)}{\Omega_1^2(q) - \Omega_2^2(q)}, \\ \tilde{G}(q) &= \frac{\Omega_1(q)Q_2[\hat{F}, \tilde{G}](q) + \Omega_2(q)Q_1[\hat{F}, \tilde{G}](q)}{\Omega_1^2(q) - \Omega_2^2(q)},\end{aligned}\tag{43}$$

where  $\tilde{G}(q) = i\hat{G}(q)$ ,  $\Omega_1(q) = \omega + 2(1 - \cos(hq) \cos(\delta h))$ ,  $\Omega_2(q) =$

$qV + 2 \sin(hq) \sin(\delta h)$  and

$$\begin{aligned}
Q_1[\hat{F}, \tilde{G}](q) &= \frac{-\gamma h^2}{4\pi^2} (\hat{F} * \hat{F} * \hat{F} - \hat{F} * \tilde{G} * \tilde{G})(q) \\
&+ \cos(\delta h) \left( \frac{(1 + \beta)h^2}{2\pi^2} \hat{F} * \hat{F} * \hat{F}_A - \frac{(1 - \beta)h^2}{2\pi^2} \tilde{G} * \tilde{G} * \hat{F}_A \right. \\
&\quad \left. - \frac{\beta h^2}{\pi^2} \hat{F} * \tilde{G} * \tilde{G}_A \right) (q) + \sin(\delta h) \left( \frac{(1 + \beta)h^2}{2\pi^2} \hat{F} * \hat{F} * \tilde{G}_B - \right. \\
&\quad \left. \frac{(1 - \beta)h^2}{2\pi^2} \tilde{G} * \tilde{G} * \tilde{G}_B - \frac{\beta h^2}{\pi^2} \hat{F} * \tilde{G} * \hat{F}_B \right) (q) \\
&+ \frac{\alpha h^2}{2\pi^2} \left( \cos(2\delta h) (\hat{F} * Q_0[\hat{F}, \tilde{G}]) \right. \\
&\quad \left. + 2 \sin(2\delta h) (\hat{F} * \hat{F}_1 * \tilde{G}_B - \hat{F} * \hat{F}_B * \tilde{G}_A) \right) (q),
\end{aligned}$$

$$\begin{aligned}
Q_2[\hat{F}, \tilde{G}](q) &= \frac{-\gamma h^2}{4\pi^2} (\hat{F} * \hat{F} * \tilde{G} - \tilde{G} * \tilde{G} * \tilde{G})(q) \\
&+ \cos(\delta h) \left( \frac{(1-\beta)h^2}{2\pi^2} \hat{F} * \hat{F} * \tilde{G}_A - \frac{(1+\beta)h^2}{2\pi^2} \tilde{G} * \tilde{G} * \tilde{G}_A \right. \\
&\left. + \frac{\beta h^2}{\pi^2} \hat{F} * \tilde{G} * \hat{F}_A \right) (q) + \sin(\delta h) \left( \frac{(1-\beta)h^2}{2\pi^2} \hat{F} * \hat{F} * \hat{F}_B - \right. \\
&\left. \frac{(1+\beta)h^2}{2\pi^2} \tilde{G} * \tilde{G} * \hat{F}_B + \frac{\beta h^2}{\pi^2} \hat{F} * \tilde{G} * \tilde{G}_B \right) (q) + \frac{\alpha h^2}{2\pi^2} \times \\
&\left( \cos(2\delta h) (\tilde{G} * Q_0[\hat{F}, \tilde{G}]) + 2 \sin(2\delta h) (\tilde{G} * \hat{F}_A * \tilde{G}_B - \tilde{G} * \hat{F}_B * \tilde{G}_A) \right) (q)
\end{aligned}$$

where  $Q_0[\hat{F}, \tilde{G}](q) = (\hat{F}_A * \hat{F}_A + \hat{F}_B * \hat{F}_B - \tilde{G}_A * \tilde{G}_A - \tilde{G}_B * \tilde{G}_B)(q)$ ,

and

$$(\hat{\mathcal{L}} * \hat{\mathcal{M}} * \hat{\mathcal{N}})(q) = \iint dq_1 dq_2 \hat{\mathcal{L}}(q_1) \hat{\mathcal{M}}(q_2) \hat{\mathcal{N}}(q - q_1 - q_2),$$

$$\hat{F}_A(q) = \hat{F}(q) \cos(qh), \hat{F}_B(q) = \hat{F}(q) \sin(qh), \tilde{G}_A(q) = \tilde{G}(q) \cos(qh), \\ \tilde{G}_B(q) = \tilde{G}(q) \sin(qh).$$

**Case 1: stationary solitary wave.** To obtain the stationary solitary wave, we set  $V = \delta = 0, \omega = \omega_s$ , and  $G = 0$ . Then the equation (41) can be reduced to the following nonlinear integral equation:

$$\hat{F}(q) = \frac{h^2}{4\pi^2\Omega(q)} [-\gamma(\hat{F} * \hat{F} * \hat{F}) + 2(1 + \beta)\hat{F} * \hat{F} * \hat{F}_A \\ + 2\alpha(\hat{F} * \hat{F}_A * \hat{F}_A + \hat{F} * \hat{F}_B * \hat{F}_B)](q) \triangleq \mathcal{K}_{\omega_s}[\hat{F}(q)], \quad (44)$$

where  $\Omega(q) = \omega_s + 2(1 - \cos(qh))$  is the frequency of the linear excitations.

Using a modified Neumann iteration scheme (Ablowitz and Biondini (Opt. Lett., 1998) and Ablowitz and Musslimani (PRE, 2002)), we construct function sequences  $\hat{F}_n(q)_{n \geq 0}$  defined by the following scheme:

$$\hat{F}_{n+1}(q) = \left| \frac{\theta(\hat{F}_n)}{v(\hat{F}_n)} \right|^{3/2} \mathcal{K}_{\omega_s}[\hat{F}_n(q)], \quad n \geq 0, \quad (45)$$

$$\theta(\hat{F}_n) = \int \hat{F}_n^2(q) dq; \quad v(\hat{F}_n) = \int \hat{F}_n(q) \mathcal{K}_{\omega_s}[\hat{F}_n(q)] dq.$$

As pointed out by Ablowitz and Musslimani (PRE, 2002), the factor

$\left| \frac{\theta(\hat{F}_n)}{v(\hat{F}_n)} \right|^l$  with  $1 < l < 2$  is introduced to stabilize the iteration scheme. Numerical simulation shows that by choosing the proper values for the parameters, then as  $n \rightarrow \infty$

$$\frac{\theta(\hat{F}_n(q))}{v(\hat{F}_n(q))} \rightarrow 1$$

and function sequences  $\hat{F}_n(q)$  is convergent. We set  $\hat{F}_n(q) \rightarrow \hat{F}_s(q)$  as  $n \rightarrow \infty$ . Then  $\hat{F}_s(q)$  is a fixed point of nonlinear integrable equation (44), and its Fourier inverse transformation  $\mathcal{F}(nh)$  is a approximate solution of Eq. (41).

Lets us give an example for the case of the following parameters

and initial  $\hat{F}_0(q)$ :

$$\alpha = -1, \beta = \gamma = \omega = 1, h = 0.5,$$

$$\hat{F}_0(q) = \operatorname{sech}(q).$$

The result of the numerical simulation is given by the following table:

$n$	$ \theta(\hat{F}_n)/v(\hat{F}_n) $	$\ \hat{F}_n - \hat{F}_s\ _{L^2}$
0	7.870361352	2.259431239
1	0.8654676779	0.5487189637
2	0.9573303456	0.1967737254
3	0.9866193377	0.07361655644
4	0.9954382285	0.02676535105
5	0.9982811553	0.007859929333
6	0.9993098242	/

Fig. 8 gives the soliton mode and describes the effect of the parameters  $\alpha, \beta, \gamma, \omega$  on soliton shape. It is interesting to note that the solitary wave has two equivalent wave peaks when  $\alpha = 10$  in fig. 8 (a).

## Case 2: traveling solitary wave.

To derive the traveling solitary wave of the dNLS equation, we employ the following modified Neumann iteration form for equation (43):

$$\begin{aligned}\hat{F}_{n+1}(q) &= \left| \frac{\theta_1(\hat{F}_n, \tilde{G}_n)}{\delta_1(\hat{F}_n, \tilde{G}_n)} \right|^{3/2} \frac{\Omega_1(q)Q_1[\hat{F}_n, \tilde{G}_n](q) + \Omega_2(q)Q_2[\hat{F}_n, \tilde{G}_n](q)}{\Omega_1^2(q) - \Omega_2^2(q)}, \\ \tilde{G}_{n+1}(q) &= \left| \frac{\theta_1(\hat{F}_n, \tilde{G}_n)}{\delta_1(\hat{F}_n, \tilde{G}_n)} \right|^{3/2} \frac{\Omega_1(q)Q_2[\hat{F}_n, \tilde{G}_n](q) + \Omega_1(q)Q_1[\hat{F}_n, \tilde{G}_n](q)}{\Omega_1^2(q) - \Omega_2^2(q)},\end{aligned}\tag{46}$$

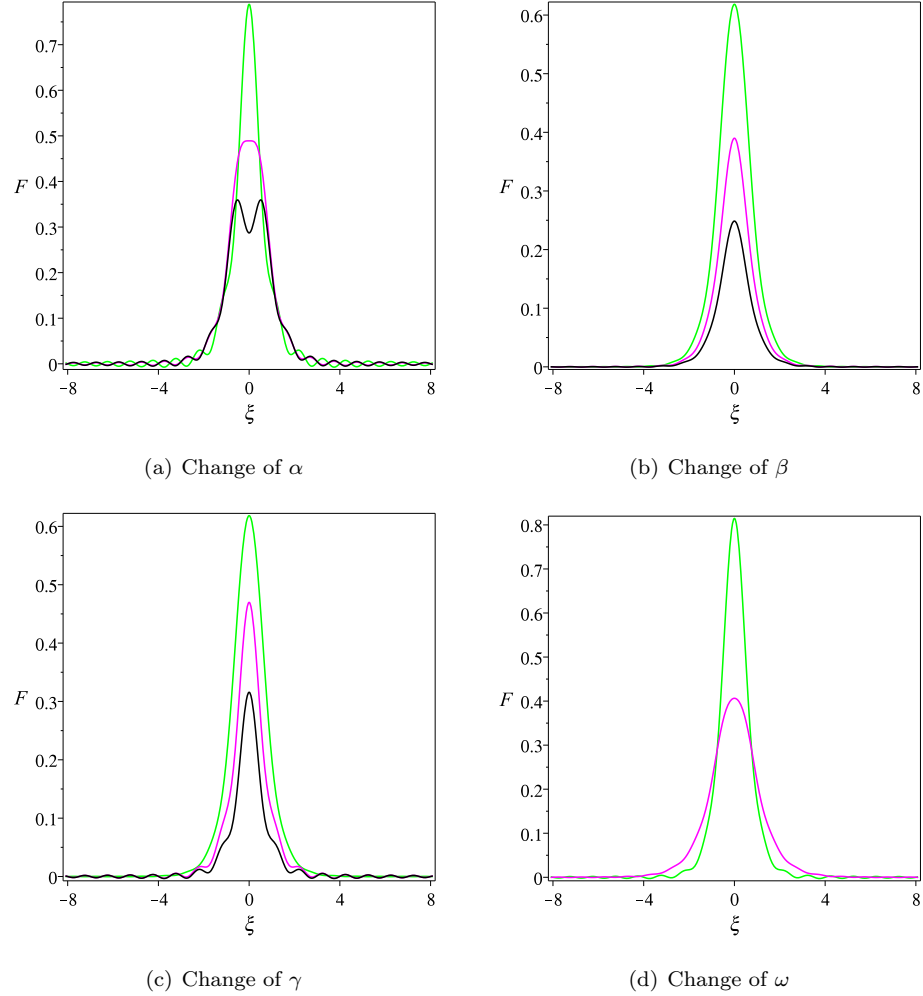


Figure 8: Mode profiles with initial value  $\hat{F}_0(q) = \text{sech}(q)$  for  $h = 0.5$  in physical space (a):  $\beta = \omega = \gamma = 1$ ,  $\alpha = -1$  (green),  $\alpha = 3$  (magenta),  $\alpha = 10$  (black) two equivalent wave peaks; (b):  $\alpha = \omega = \gamma = 1$ ,  $\beta = 1$  (green),  $\beta = 6$  (magenta),  $\beta = 18$  (black); (c) leap property:  $\alpha = \omega = \beta = 1$ ,  $\gamma = 1$  (green),  $\gamma = 6$  (magenta),  $\gamma = 18$  (black); (d):  $\alpha = \beta = \gamma = 1$ ,  $\omega = 1.5$  (green),  $\omega = 0.5$  (magenta).

where

$$\begin{aligned}
\theta_1 &= \int \left( \hat{F}_n^2(q) + \tilde{G}_n^2(q) \right) dq, \\
\delta_1 &= \int \frac{1}{\Omega_1^2(q) - \Omega_2^2(q)} \left\{ \hat{F}_n(q) \left( \Omega_1(q) Q_1[\hat{F}_n, \tilde{G}_n](q) + \Omega_2(q) Q_2[\hat{F}_n, \tilde{G}_n](q) \right) \right. \\
&\quad \left. + \tilde{G}_n(q) \left( \Omega_1(q) Q_2[\hat{F}_n, \tilde{G}_n](q) + \Omega_2(q) Q_1[\hat{F}_n, \tilde{G}_n](q) \right) \right\} dq.
\end{aligned} \tag{47}$$

Similar to the case of stationary solitary wave, by numerical simulation, as  $n \rightarrow \infty$ , we have

$$\frac{\theta_1(\hat{F}_n, \tilde{G}_n)}{\delta_1(\hat{F}_n, \tilde{G}_n)} \rightarrow 1,$$

and function sequences  $\hat{F}_n(q)$  and  $\tilde{G}_n(q)$  are convergent. We set

$\hat{F}_n(q) \rightarrow \hat{F}_s(q)$  and  $\tilde{G}_n(q) \rightarrow \tilde{G}_s(q)$  as  $n \rightarrow \infty$ . Then  $\hat{F}_s(q), \tilde{G}_s(q)$  is a fixed point of nonlinear integrable equation (43), and their Fourier inverse transformation  $\mathcal{F}(nh), \mathcal{G}(nh)$  is a approximate solution of Eq. (41). Let us give a numerical simulation for the case of the following parameters and initial functions:

$$\alpha = 2, \beta = 0.5, \gamma = 1, \omega = 1, h = 0.5, v = -0.25, \delta = 0.5,$$

$$\hat{F}_0(q) = \operatorname{sech}(q), \quad \tilde{G}_0(q) = \operatorname{sech}(q) \tanh(q).$$

The following table gives the result of the numerical simulation:

$n$	$ \theta_1(\hat{F}_n, \tilde{G}_n)/\delta_1(\hat{F}_n, \tilde{G}_n) $	$\ \hat{F}_n - \hat{F}_s\ _{L^2}$	$\ \hat{G}_n - \hat{G}_s\ _{L^2}$
0	5.821356102	2.281272518	0.8568407788
1	0.8226148954	0.4123725698	1.229177002
2	0.9700214726	0.3184335813	0.6361060322
3	0.9973277869	0.2508873299	0.3521664710
4	0.9994003139	0.1829277594	0.1960756501
5	0.9992797673	0.1277556029	0.1089196004
6	0.9991680137	0.08687764605	0.06063248271
7	0.9991812547	0.05790679463	0.03394770281
8	0.9992867774	0.03785790219	0.01912434510
9	0.9994309015	0.02418053795	0.01079248505

10	0.9995737753	0.01493796539	0.006031421443
11	0.9996957398	0.008733876954	0.003258313085
12	0.9997913302	0.004589589679	0.001610932003
13	0.9998623747	0.001831145764	0.0006137772628
14	0.9999133525	/	/

Fig. 9 gives the shape of the solitary wave in physical space with initial values  $\hat{F}_0(q) = \text{sech}(q)$ ,  $\tilde{G}_0(q) = \text{sech}(q) \tanh(q)$  and parameters  $\alpha = 2$ ,  $\beta = 0.5$ ,  $\gamma = 1$ ,  $\omega = 1$ ,  $h = 0.5$ ,  $v = -0.25$ ,  $\delta = 0.5$ .

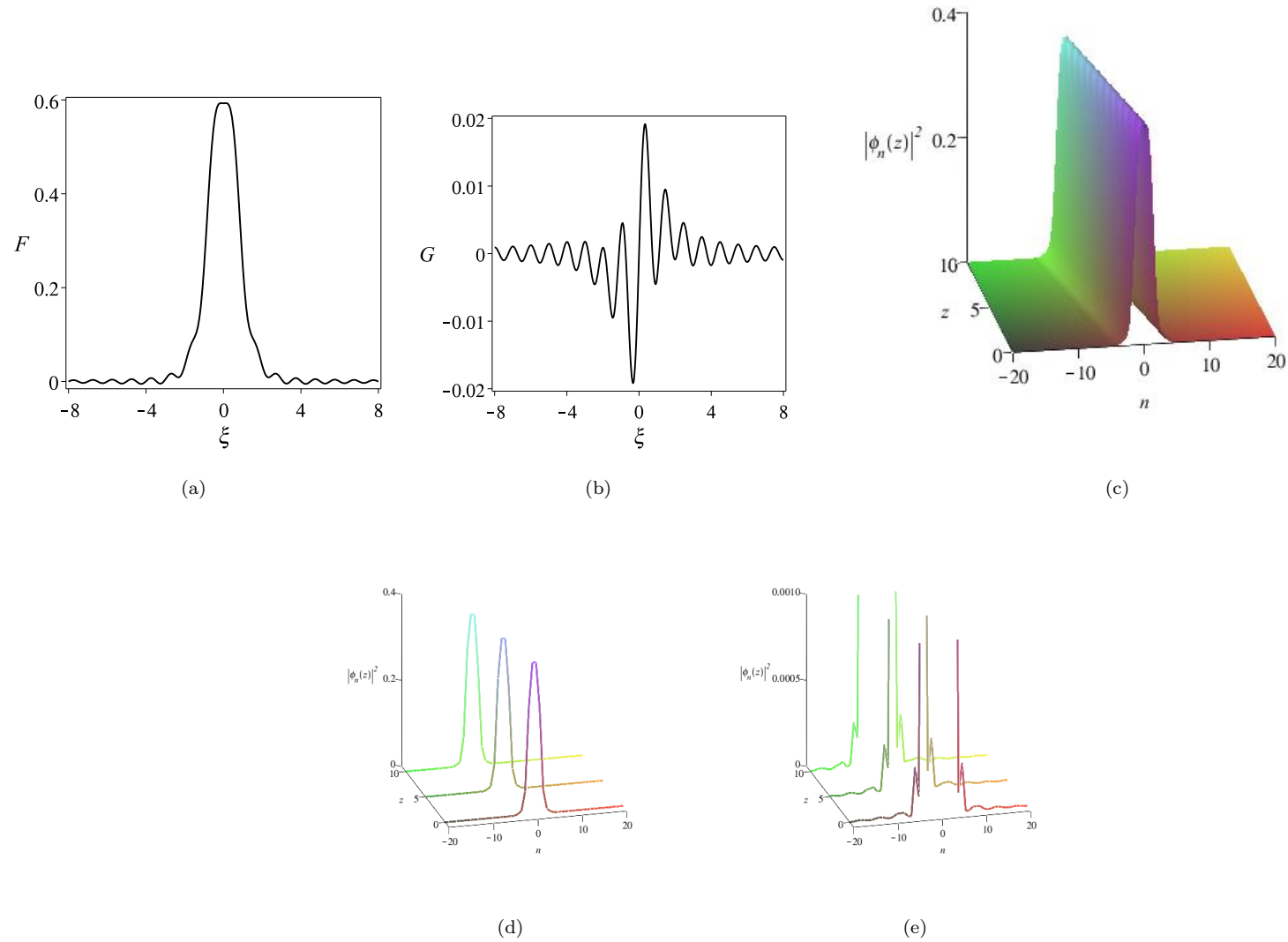


Figure 9: Soliton shape with initial values  $\hat{F}_0(q) = \text{sech}(q)$ ,  $\tilde{G}_0(q) = \text{sech}(q) \tanh(q)$  in physical space for  $\alpha = 2, \beta = 0.5, \gamma = 1, \omega = 1, h = 0.5, V = -0.25, \delta = 0.5$ .

## 4. Conclusions

- By using the plane map approach, we have addressed the spatial properties of nonintegrable dNLS equation (4).
- By using discrete Fourier transformation method, we have obtained numerical approximations of stationary and travelling solitary wave solutions of the nonintegrable discrete NLS equation.

**THANK YOU**